NANO LETTERS
Cite This: Nano Lett. 2019, 19, 8381−8387
Letter
pubs.acs.org/NanoLett

Emergent Magnetic State in (111)-Oriented Quasi-Two-Dimensional Spinel Oxides

Xiaoran Liu,*[,†] Sobhit Singh,[†] Brian J. Kirby,[‡] Zhicheng Zhong,[¶] Yanwei Cao,[¶] Banabir Pal,[†] Mikhail Kareev,[†] Srimanta Middey,[§] John W. Freeland,[∥] Padraic Shafer,[⊥] Elke Arenholz,[⊥] David Vanderbilt,[†] and Jak Chakhalian[†]

[†]Department of Physics and Astronomy, Rutgers University, Piscataway, New Jersey 08854, United States
[‡]NIST Center for Neutron Research, National Institute of Standards and Technology, Gaithersburg, Maryland 20899, United States
[¶]Ningbo Institute of Materials Technology and Engineering, Chinese Academy of Sciences, Ningbo, Zhejiang 315201, China
[§]Department of Physics, Indian Institute of Science, Bengaluru 560012, India
[∥]Advanced Photon Source, Argonne National Laboratory, Argonne, Illinois 60439, United States
[⊥]Advanced Light Source, Lawrence Berkeley National Laboratory, Berkeley, California 94720, United States

Supporting Information

ABSTRACT: We report on the emergent magnetic state of (111)-oriented $CoCr_2O_4$ ultrathin films sandwiched between Al_2O_3 spacer layers in a quantum confined geometry. At the two-dimensional crossover, polarized neutron reflectometry reveals an anomalous enhancement of the total magnetization compared to the bulk value. Synchrotron X-ray magnetic circular dichroism measurements demonstrate the appearance of a long-range ferromagnetic ordering of spins on both Co and Cr sublattices. Brillouin function analyses and ab-initio density functional theory calculations further corroborate that the observed phenomena are due to the strongly altered magnetic frustration invoked by quantum confinement effects, manifested by the onset of a Yafet−Kittel-type ordering as the magnetic ground state in the ultrathin limit, which is unattainable in the bulk.

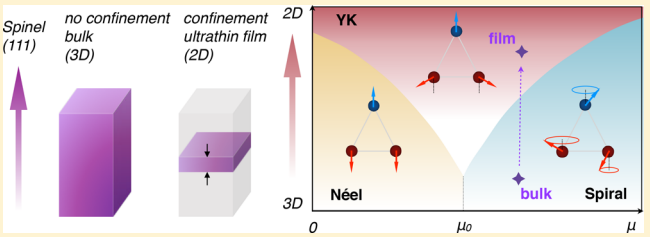

KEYWORDS: *Spinels, ultrathin films, emergent properties, magnetism*

The quest to design, discover, and manipulate new quantum states of matter has fostered tremendous research activity among condensed matter physicists. Recent progress in the fabrication of epitaxial thin films has empowered this effort with additional means and led to a plethora of interesting artificial multilayers and heterostructures grown with atomic level of precision.[1−4] Nowadays, the interest to realize exotic physics linked to many-body phenomena has shifted to tailoring the magnetic states in quasi-two-dimensional (2D) limit.[5,6] On one hand, according to the Mermin−Wagner theorem, in an isotropic Heisenberg spin system of dimensionality $D \leq 2$, enhanced thermal fluctuations prohibit the onset of a long-range (ferro- or antiferro-) magnetic ordering at any finite temperature.[7] On the other hand, lowering the dimensionality brings about several new factors that can radically alter a quantum system owing to changes in band topology, ionic coordinations and covalency, crystal fields, exchange pathways, magnetic anisotropy, quantum confinement, and universality class.[2,8−13] As a result, in the crossover to low dimensions, the magnetic ground state of a material can be distinctly different from its three-dimensional (3D) counterpart, thus opening a plethora of opportunities for emergent or hidden materials phases.

In this context, it is interesting to ask whether one can "dial-in" dimensionality of a system from 3D to 2D in a controllable way, and what can happen to the quantum state when the low dimensionality entwines with frustration? Here, we remind that the frustrated magnets are systems where the localized spins are entangled in an incompatible way due to either multiple competing exchange interactions or the underlaying lattice geometry or both.[14−18] Generally, frustration tends to suppress the spin ordering and promotes a complex magnetic phase diagram typically with a set of competing ground states.[19] Furthermore, a large number of theoretical proposals have recently addressed another aspect showing how dimensionality effectively tunes the many-body effects, either driving the ground state into an entirely different regime on the magnetic phase diagram or inducing unconventional phases through quantum criticality.[19−21]

Received: May 27, 2019
Revised: September 29, 2019
Published: October 30, 2019

DOI: 10.1021/acs.nanolett.9b02159
Nano Lett. 2019, 19, 8381−8387

Among many magnetically frustrated compounds, the family of chromate spinels MCr_2O_4 (M = Mn, Fe, and Co) has attracted intense interest.[22−40] These materials crystallize into the normal spinel structure AB_2O_4, with M^{2+} and Cr^{3+} ions occupying the tetrahedral (A) and octahedral (B) sites, respectively. As both the nearest-neighbor exchange interactions J_{AB} and J_{BB} are antiferromagnetic (see Figure 1c), a strong competition between the exchange interactions ($J_{BB}/J_{AB} > 2/3$) causes magnetic frustration, resulting in a unique three-sublattice ferrimagnetic spiral order.[41,42] In the bulk, such a conical spiral order engenders a macroscopic spontaneous polarization which is switchable by an external magnetic field,[43−45] consistent with the calculations based on the spin-current model[46] and the inverse Dzyaloshinskii−Moriya interaction model.[47]

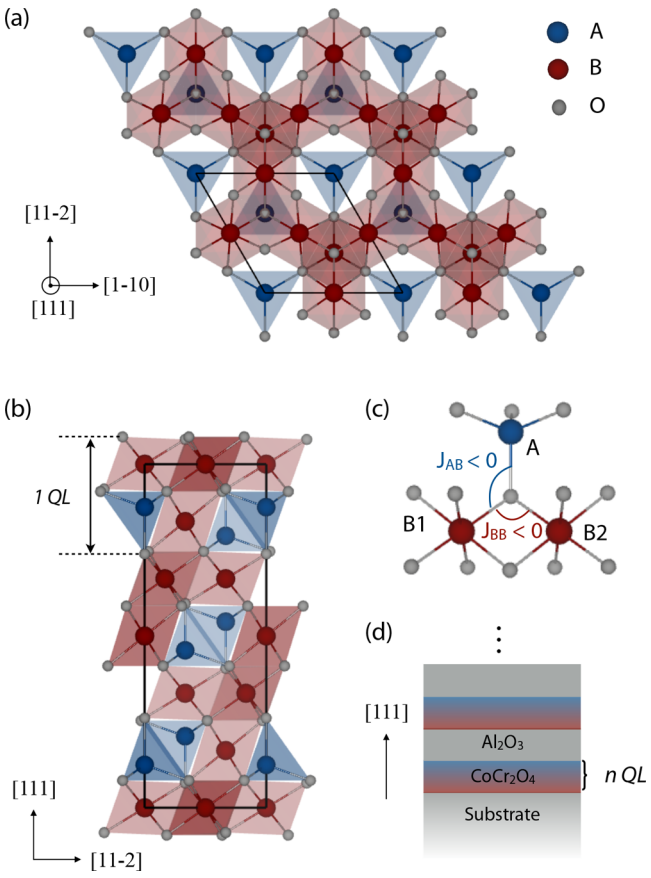

Figure 1. (a) Crystal structure of normal spinel AB_2O_4 viewed along [111] direction. The oxygen ions stack in the cubic close-packed framework, forming both tetrahedral and octahedral interstitials, which are separately occupied by A and B cations. (b) View of the structure along the [1−10] direction. (c) Nearest-neighbor exchange interactions in normal spinels with magnetic A and B ions. Both J_{AB} and J_{BB} are antiferromagnetic, leading to magnetic frustration. (d) Schematic of the ultrathin (111)-oriented $CoCr_2O_4$ thin films confined between Al_2O_3 spacers.

Strikingly, when viewed along the [111] direction, the spinel crystal structure shows a stacking of triangular and Kagome cation planes with intrinsically large geometrical frustration (GF), embedded in the oxygen cubic close-packed frame, as illustrated in Figure 1a,b. Specifically, in this viewpoint, the basic structural arrangement is "$-O_4-B_3-O_4-A-B-A-$", containing four cation layers, which we denote as one quadruplet layer or QL. Therefore, we may speculate that if the lattice can be confined along such a GF direction, the magnetic frustration will be strongly altered, which could potentially lead to the formation of emergent magnetic phases in quasi-2D. Naturally, the thin-film approach offers a direct access to the modalities for manipulation and control of these phases.

Based on the above-mentioned framework, we demonstrate the power of the proposed approach for magnetic ground-state manipulation in the prototypical case of $CoCr_2O_4$ spinel layered along [111] direction. In bulk $CoCr_2O_4$, the ground state has a three-sublattice ferrimagnetic spiral configuration with the onset of ferrimagnetism at $T_C \sim 93$ K, and the incommensurate spin-spiral order at $T_S \sim 26$ K.[42,48] The incommensurate to commensurate lock-in transition further takes place at $T_L \sim 14$ K.[49] In this Letter, we report on the discovery of an emergent magnetic state in (111)-oriented $CoCr_2O_4$ ultrathin films confined by inert Al_2O_3 layers. Spin polarized neutron reflectivity (PNR) confirms the establishment of long-range magnetic ordering in $CoCr_2O_4$ slabs with thickness of few nanometers only. Importantly, analysis on the X-ray magnetic circular dichroism (XMCD) data reveals that even though the magnetic ordering of these quasi-2D films is still ferrimagnetic, it is no longer of the spin-spiral type, but rather the Yafet−Kittel type, which was theoretically proposed[50] but never realized in the bulk phase diagram of $CoCr_2O_4$.

The (111)-oriented $[n\text{QL } CoCr_2O_4/1.3 \text{ nm } Al_2O_3]_4$ superlattices (1QL ≈ 0.48 nm; n = 4, 2) were fabricated by pulsed laser deposition on single crystalline (0001)-oriented Al_2O_3 substrate, as sketched in Figure 1d. The α-Al_2O_3 was selected as the nonmagnetic confinement spacer because of the good structural compatibility with $CoCr_2O_4$.[51] Details of the materials synthesis, structural and chemical characterizations are given elsewhere.[51,52] Additionally, the degree of cation distribution disorder is investigated by resonant X-ray absorption spectroscopy (XAS). Within the experimental limit, no signs of cation distribution disorder or ion valency change is observed for all samples. Specifically, the obtained absorption line-shapes as well as the absorption energy peak positions at the $L_{3,2}$ absorption edges of both Co and Cr are practically identical to that of the bulk $CoCr_2O_4$ reference.[10] These results further confirm that the ultrathin heterostructures are of expected thickness, orientation, and proper local chemical environments.

First, we discuss the presence of the net magnetization in the (111)-oriented superlattices and compare it to a bulk-like $CoCr_2O_4$ (50 QL, 24 nm) sample. In order to probe the rather small magnetic signals in the superlattices, we performed the PNR experiments at the PBR beamline at the NIST Center for Neutron Research. The polarized neutron beam was set incident at a grazing angle, and the specular reflectivity was recorded as a function of the transfer wave vector Q_z along the surface normal. In general, PNR provides sensitivity to the nuclear and magnetic depth profiles. However, in this case, our real-space resolution is limited by signal-to-noise limitations that prevented us from measuring out to a Q_z value corresponding to the superlattice periodicity (i.e., the first Bragg peak). Nevertheless, by employing a highly constrained model based on data from other measurements, model fits to the data provide exquisite sensitivity to the relatively weak magnetization of our samples. Specifically in our model, we fix the individual layer thickness and roughness values to be those

DOI: 10.1021/acs.nanolett.9b02159
Nano Lett. 2019, 19, 8381−8387

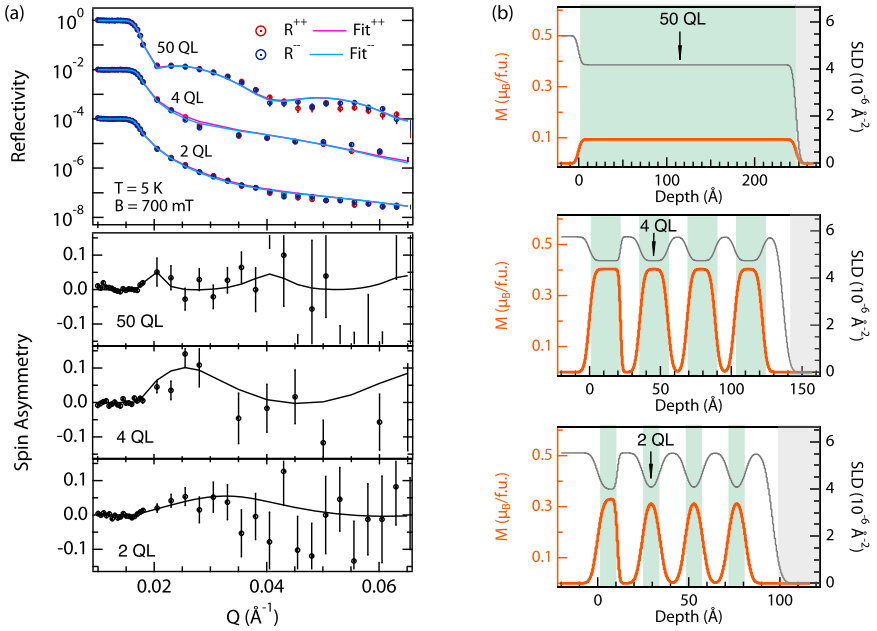

Figure 2. (a) Non-spin-flip PNR data with model fitting for both $CoCr_2O_4$ thick film (50 QL) and ultrathin $[n\text{QL } CoCr_2O_4/1.3 \text{ nm } Al_2O_3]_4$ superlattices, plotted as reflectivity and spin asymmetry, respectively. Reflectivity curves are offset in intensity for clarity of presentation. Spin asymmetry is defined as $(R^{++} - R^{--})/(R^{++} + R^{--})$. All data were measured at 5 K under 0.7 T in-plane magnetic field. (b) Depth profiles of the net magnetization (M) and the nuclear scattering length density (SLD). The regions in light green denote the $CoCr_2O_4$ slabs inside the sample, and the gray regions denote air on top of the sample surface.

determined from X-ray reflectivity measurements that extend to much higher Q_z[51] and assume that the Al_2O_3 layers exhibit zero magnetization. The fitting was performed using the NIST Refl1D[53] software routines.

Figure 2a,b presents the fitted PNR data, along with the model profiles corresponding to the fits. The lower panels of (a) show the fitted data plotted as spin asymmetry (the difference in R^{++} and R^{--} divided by the sum). Since the sample magnetization manifests as splitting of the R^{++} and R^{--} reflectivity, the nonzero spin asymmetry observed for all three samples indicates sensitivity to the underlying magnetic order in the samples. Note, since during the measurements we applied only a moderate magnetic field of 0.7 T, the fitted values of M imply the presence of a spontaneous long-range magnetization rather than canting of the local moment in a paramagnetic phase. First, the validity of the model is tested on the 50 QL thick film, which yields $M = (0.10 \pm 0.02)\ \mu_B$/f.u. very close to the reported value in bulk $CoCr_2O_4$ with the spiral spin state.[44] Intriguingly, in the ultrathin case the magnitude of M becomes remarkably *enhanced*, reaching $(0.39 \pm 0.03)\ \mu_B$/f.u. in 4 QL and $(0.31 \pm 0.08)\ \mu_B$/f.u. in 2 QL samples, respectively. To appreciate this result, we emphasize that even in the bulk, the saturated magnetization from the collinear component of the spiral order can reach only ∼0.15 μ_B/f.u.[43,44] This strongly suggests that the nearly 4-fold increase of M in 4 QL and 2 QL films cannot be attributed to mundane changes in magnetic anisotropy with thickness. Instead, these findings imply the presence of a more fundamental modification of the magnetic structure which takes place in the quasi 2D limit of the (111)-oriented ultrathin films.

In order to elucidate the magnetic structure of each sublattice, we performed resonant XAS measurements with left- and right-circularly polarized beams at beamline 4.0.2 of the Advanced Light Source at Lawrence Berkeley National Laboratory. The spectra were measured at 15 K under 0.1 T magnetic field and recorded using the luminescence detection mode. The circularly polarized X-rays were incident with an angle of 30° relative to the sample surface. The intensities were normalized with respect to their corresponding absorption spectra. The difference between these two spectra, known as the XMCD, originates from the local magnetization of a specifically probed chemical element (i.e., Co or Cr). The XMCD results at Co and Cr $L_{3,2}$ edges are shown in Figure 3a. The dichroic signals of similar line shape are clearly evident for all samples on both elements. Moreover, the sign of the XMCD spectra is opposite for Co and Cr, as observed at the strongest feature near their L_3 edge (Cr at ∼577 eV and Co at ∼778 eV), signifying that the spin orientation on Cr ions is antiparallel to that of the Co ions. To quantify the values of the orbital and spin magnetic moments on each element, we applied the "sum rules" analysis to the spectra.[54−56] In particular, to compensate for the spectral overlap of Cr L_3 and L_2 transitions, the spin magnetic moment of Cr deduced from the spin sum rule has been corrected by the spin correction factor[57] (see Supporting Information).

The obtained results are summarized in Table 1. As seen, for all samples the magnetic moment of Co dominates over the magnetic moment of Cr and determines the overall direction of the net magnetization (M_{net}). In addition, M_{net} exhibits strong enhancement from ∼0.10 μ_B/f.u. in 50 QL to ∼0.23 μ_B/f.u. in 4 QL, but reduces back to ∼0.13 μ_B/f.u. in 2 QL. We note the values of net magnetization obtained from XMCD are all relatively smaller than their counterparts from PNR measurements, which is likely due to the difference of magnetic domains within the materials. Since the PNR was measured after cooling the samples in 0.7 T magnetic field, while the XMCD was measured in 0.1 T after zero field cooling process, more of the magnetic domains were aligned during the PNR experiments, leading to larger net magnetizations.

DOI: 10.1021/acs.nanolett.9b02159
Nano Lett. 2019, 19, 8381−8387

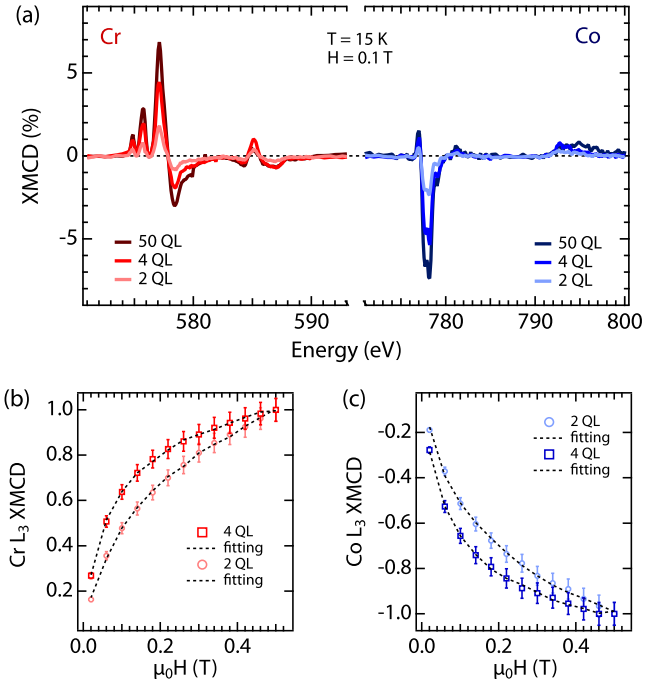

Figure 3. (a) Cr and Co $L_{2,3}$ edges XMCD data of (111)-oriented $CoCr_2O_4$ thin films of various thickness. (b, c) Field-dependent XMCD results of n = 4 and 2 QL samples taken at Cr and Co L_3 maximal peak positions (Cr at ∼577 eV; Co at ∼778 eV) with the Brillouin function fittings.

Table 1. Magnetic Moment of Each Element (Co^{2+} and Cr^{3+}) of All Samples (n = 50, 4, and 2 QL) Obtained from XMCD Sum Rules[a]

n (QL)	M_{Co} (μ_B/Co^{2+})	M_{Cr} (μ_B/Cr^{3+})	M_{net} (μ_B/f.u.)
50	0.65	−0.28	0.10
4	0.64	−0.22	0.23
2	0.26	−0.074	0.13

[a]The net moment per $CoCr_2O_4$ formula unit (f.u.) is calculated as $M_{net} = (M_{Co} + 2M_{Cr})/\cos 30°$, where a factor of cos 30° is included to account for the incident angle of x-rays.

Nevertheless, the nonmonotonic trend of M vs n is qualitatively similar in both XMCD and PNR characterizations. Together these observations affirm that even in the ultrathin limit, the ground state is indeed ferrimagnetic.

Next, we turn our attention to the spin configuration of the ferrimagnetic state in (111) $CoCr_2O_4$ ultrathin films. For this purpose, we recorded the XMCD intensity of each element as a function of applied magnetic field at the maximal absorption peak position (i.e., 577 eV for Cr and 778 eV for Co) (see Figure 3b,c). While in the bulk it has been demonstrated that $CoCr_2O_4$ has a conical spiral spin configuration with the net magnetization contributed from three different sublattices (Co, Cr1, and Cr2), here, we find that our field-dependent XMCD data are reconciled with a new magnetic ground state described by a two-sublattice ferrimagnetic model.[58,59] Specifically, unlike bulk, in the 2D limit, the Cr1 and Cr2 sites contribute equally to the net magnetization, and the spins on the remaining two magnetic sublattices of Co and Cr align antiparallel to each other. Within the nearest-neighbor approximation, the Weiss molecular field on each site has contributions from both the intersublattice ($J_{Co\text{-}Cr}$) and the intrasublattice ($J_{Co\text{-}Co}$ and $J_{Cr\text{-}Cr}$) exchange interactions. The ratio $J_{Co\text{-}Cr}/J_{Cr\text{-}Cr}$, which is a reflection of the degree of frustration, can be extracted by fitting the field-dependent XMCD data to the modified Brillouin function of this model.[60]

According to the theory proposed by Lyons, Kaplan, Dwight, and Menyuk (LKDM),[42] in a normal spinel compound, the parameter $\mu = 4J_{BB}S_B/3J_{AB}S_A$ determines spin configuration of the ground state. In particular, the ground state is a two-sublattice Néel-type collinear ferrimagnet for $\mu <$ 0.89 but turns into a three-sublattice spiral ferrimagnet for 0.89 $< \mu <$ 1.30. Larger values of μ indicate further enhancement of the magnetic frustration that renders the spiral ordering unstable. In our case, the Brillouin function fitting yields the experimental values of $\mu \approx$ 0.64 for 4 QL and 0.49 for 2 QL, respectively. As a result, the frustration effect should have been reduced ($\mu \approx$ 2 in bulk),[48] shifting the magnetic ground state from the region of spiral ferrimagnet (with the propagation vector along the [110] direction)[48] to Néel-type ferrimagnet. In fact, in the ultrathin-film geometry, the confinement along the [111] direction also breaks the translational symmetry along [110] and naturally prevents the onset of the spiral long-range order. However, the ground state cannot hold the Néel-type collinear ferrimagnetic configuration either as it would have required a net magnetization of ∼3μ_B/f.u. with the overall direction following the Cr sublattice. This type of ordering is clearly in sharp variance with the observed XMCD results which show a rather small net magnetization with the direction aligned along the Co sublattice.

To understand what kind of magnetic ordering emerges in the ultrathin case, we recall that for an intermediate magnitude of frustration on a normal spinel lattice, Yafet and Kittel (YK) proposed another ground state which deviates from the Néel collinear configuration.[50] As illustrated in Figure 4, in this

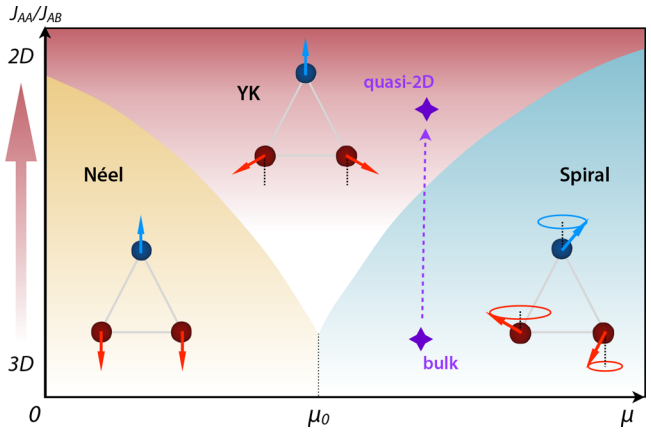

Figure 4. Extended phase diagram including μ, the relative strength of J_{AA}/J_{AB}, and the magnetic ground state in (111) cubic normal spinel films. The findings on $CoCr_2O_4$ are illustrated by the purple diamonds on the figure, based on the DFT results.

model, the spins on the B site are divided in two groups, each group has spins canting in an opposite way but at the same angle α_{YK} relative to the net magnetization direction. According to the YK theory, the magnitude of the canting angle α_{YK} is determined by the strength of frustration. The Néel-type collinear configuration is the special case of $\alpha_{YK} = 0$.

In the following, we speculate on a possible mechanism for the stabilization of the YK spin configuration in (111)-oriented $CoCr_2O_4$ ultrathin films. First, we note that in general the YK configuration can be triggered due to structural "imperfection"

DOI: 10.1021/acs.nanolett.9b02159
Nano Lett. 2019, 19, 8381−8387

of a spinel compound, that is, the existence of tetragonal distortion,[61−64] cation distribution disorder,[65] or inclusion of higher order exchange interactions.[66] For our samples, tetragonal distortion can be ruled out as the films are grown along the three-fold symmetry axis. The distortion if present should be of the trigonal type, rather than tetragonal type, which will induce slight variation of the cation−oxygen−cation bond angles, but keep the bond lengths the same.[67,68] Moreover, the existence of finite cation distribution disorder is excluded by our XAS results. Therefore, we suggest that the YK state is likely stabilized due to the activation of additional exchange interactions. In particular, it has been pointed out from a recent first-principles study that the exchange coupling between A sites may not be necessarily negligible, as was initially assumed in the LKDM theory.[69] Obviously, inclusion of non-negligible J_{AA} can further enhance the magnetic frustration and destabilize the collinear Néel configuration.

To verify this speculation, we performed first-principles density functional theory (DFT) calculations to determine the exchange interactions (J_{ij}^{N}, N = 1, 2 for the first and second nearest-neighbor interactions, respectively) in both bulk $CoCr_2O_4$ and n = 2 superlattices. The calculations reveal that the first nearest-neighbor J_{AB}^{1} is the leading exchange term in bulk as well as in n = 2 case, followed by the J_{BB}^{1} term. Compared to bulk, the strength of all exchange terms increases to some extent in n = 2. But notably, the J_{AA}^{1} term has the most significant enhancement by ∼6 times from 0.70 to 4.16 meV, which tends to increase the magnetic frustration within the A sublattice (see Supporting Information for more details). This is consistently evident by comparing the relative strength of the exchange terms to J_{AB}^{1}. As shown in Table 2, the ratio of J_{AA}^{1}/J_{AB}^{1} increases from 0.14 in bulk to 0.34 in n = 2, which becomes comparable to the ratio of J_{BB}^{1}/J_{AB}^{1}. These results confirm as the dimension of $CoCr_2O_4$ is reduced to quasi-2D, the J_{AA}^{1} term that was "dormant" in bulk is effectively activated, consistent with our speculation.

Table 2. Relative Strength of Each Exchange Interaction to J_{AB}^{1} in Both Bulk and n = 2 $CoCr_2O_4$[a]

J_{ij}^{N}	J_{ij}^{N}/J_{AB}^{1} (bulk)	J_{ij}^{N}/J_{AB}^{1} (n = 2)
J_{AB}^{1}	1	1
J_{BB}^{1}	0.43	0.52
J_{AA}^{1}	0.14	0.34
J_{AB}^{2}	−0.13	−0.08
J_{BB}^{2}	−0.01	−0.04

[a]The positive values denote antiferromagnetic (AFM) exchange interactions, whereas negative values denote ferromagnetic (FM) exchange interactions.

Based on above discussion, we propose an extended magnetic phase diagram which now includes the YK spin configuration for (111) cubic normal spinel films as a function of μ and J_{AA}/J_{AB}, to reflect the propensity toward 2D. As illustrated in Figure 4, the magnetism of both bulk compounds and thick films still qualitatively follows the conventional LKDM theory with the magnetic ground state of either Néel or the spiral type, separated by a critical μ_0. Nevertheless, the value of μ_0 may deviate from 0.89 with the inclusion of J_{AA}. Application of confinement along the [111] direction effectively activates and enhances the relative strength of J_{AA}/J_{AB}, driving the system along the vertical axis to the intermediate regime, where the YK state eventually emerges at the quasi-2D limit. To further experimentally explore this phase space, in addition to our findings on $CoCr_2O_4$, future work using other spinel compounds with a Néel type configuration in bulk can help to map out the complete phase diagram.

In summary, we report on the discovery of an emergent magnetic state in quasi-2D (111)-oriented $CoCr_2O_4$ ultrathin films. Upon the dimensionality reduction along the [111] direction, the subtle interplay among multiple exchange interactions is markedly altered, and the system shifts into the intermediate region of the extended magnetic phase diagram. As a consequence of the quantum confinement and the activated higher-order exchange interactions, a hidden Yafet−Kittel spin configuration takes over the spiral one as the ground state. Our findings highlight the utility of dimensionally control and designed lattice topology toward realizing novel magnetic states inaccessible in the bulk.

■ ASSOCIATED CONTENT

Supporting Information

The Supporting Information is available free of charge on the ACS Publications website at DOI: 10.1021/acs.nanolett.9b02159.

Additional information regarding PNR measurements, XMCD sum rules analyses, Brillouin function fittings, and DFT calculations (PDF)

■ AUTHOR INFORMATION

Corresponding Author

*Email: xiaoran.liu@rutgers.edu.

ORCID

Xiaoran Liu: 0000-0003-0938-6109
Zhicheng Zhong: 0000-0003-1507-4814
Srimanta Middey: 0000-0001-5893-0946
Padraic Shafer: 0000-0001-9363-2557

Notes

The authors declare no competing financial interest.

■ ACKNOWLEDGMENTS

The authors thank D. Khomskii, G. Fiete, X. Hu, D. D. Sarma, and P. Mahadevan for numerous insightful discussions. X.L. and J.C. were supported by the Gordon and Betty Moore Foundation's EPiQS Initiative through grant GBMF4534 and by the Department of Energy under grant DE-SC0012375. S.S. and D.V. acknowledge the support from ONR grants N00014-16-1-2951 and N00014-17-1-2449. This research used resources of the Advanced Light Source, which is a Department of Energy Office of Science User Facility under contract no. DE-AC02-05CH11231. This research used resources of the Advanced Photon Source, a U.S. Department of Energy Office of Science User Facility operated by Argonne National Laboratory under contract no. DE-AC02-06CH11357.

■ REFERENCES

(1) Schlom, D.; Chen, L.; Eom, C.; Rabe, K.; Streiffer, S.; Triscone, J. Strain tuning of ferroelectric thin films. *Annu. Rev. Mater. Res.* **2007**, *37*, 589−626.

(2) Hwang, H. Y.; Iwasa, Y.; Kawasaki, M.; Keimer, B.; Nagaosa, N.; Tokura, Y. Emergent phenomena at oxide interfaces. *Nat. Mater.* **2012**, *11*, 103−113.

DOI: 10.1021/acs.nanolett.9b02159
Nano Lett. 2019, 19, 8381−8387

(3) Stemmer, S.; Allen, J. S. Two-dimensional electron gases at complex oxide interfaces. *Annu. Rev. Mater. Res.* **2014**, *44*, 151−171.
(4) Bhattacharya, A.; May, S. J. Two-dimensional electron gases at complex oxide interfaces. *Annu. Rev. Mater. Res.* **2014**, *44*, 65−90.
(5) Coey, J.M.D.; Ariando; Pickett, W.E. Magnetism at the edge: New phenomena at oxide interfaces. *MRS Bull.* **2013**, *38*, 1040−1047.
(6) Hellman, F.; Hoffmann, A.; Tserkovnyak, Y.; Beach, G.; Fullerton, E.; Leighton, C.; MacDonald, A. H.; Ralph, D. C.; Arena, D. A.; Dürr, H. A.; Fischer, P.; Grollier, J.; Heremans, J. P.; Jungwirth, T.; Kimel, A. V.; Koopmans, B.; Krivorotov, I. N.; May, S. J.; Petford-Long, A. K.; Rondinelli, J. M.; Samarth, N.; Schuller, I. K.; Slavin, A. N.; Stiles, M. D.; Tchernyshyov, O.; Thiaville, A.; Zink, B. L. Interface-induced phenomena in magnetism. *Rev. Mod. Phys.* **2017**, *89*, No. 025006.
(7) Mermin, N. D.; Wagner, H. Absence of ferromagnetism or antiferromagnetism in one or two-dimensional isotropic Heisenberg models. *Phys. Rev. Lett.* **1966**, *17*, 1133−1136.
(8) Bansil, A.; Lin, H.; Das, T. Colloquium: Topological band theory. *Rev. Mod. Phys.* **2016**, *88*, No. 021004.
(9) Chakhalian, J.; Freeland, J. W.; Millis, A. J.; Panagopoulos, C.; Rondinelli, J. M. Colloquium: Emergent properties in plane view: Strong correlations at oxide interfaces. *Rev. Mod. Phys.* **2014**, *86*, 1189−1202.
(10) Liu, X.; Middey, S.; Cao, Y.; Kareev, M.; Chakhalian, J. Geometrical lattice engineering of complex oxide heterostructures: a designer approach to emergent quantum states. *MRS Commun.* **2016**, *6*, 133−144.
(11) Song, C.; You, Y.; Chen, X.; Zhou, X.; Wang, Y.; Pan, F. How to manipulate magnetic states of antiferromagnets. *Nanotechnology* **2018**, *29*, 112001.
(12) Ueda, K.; Tabata, H.; Kawai, T. Ferromagnetism in $LaFeO_3$-$LaCrO_3$ superlattices. *Science* **1998**, *280*, 1064−1066.
(13) Chen, Y. Z.; Bovet, N.; Trier, F.; Christensen, D. V.; Qu, F. M.; Andersen, N. H.; Kasama, T.; Zhang, W.; Giraud, R.; Dufouleur, J.; Jespersen, T. S.; Sun, J. R.; Smith, A.; Nygård, J.; Lu, L.; Büchner, B.; Shen, B. G.; Linderoth, S.; Pryds, N. A high-mobility two-dimensional electron gas at the spinel/perovskite interface of γ-Al_2O_3/$SrTiO_3$. *Nat. Commun.* **2013**, *4*, 1371.
(14) Ramirez, A. P. Strongly geometrically frustrated magnets. *Annu. Rev. Mater. Sci.* **1994**, *24*, 453−480.
(15) Greedan, J. E. Geometrically frustrated magnetic materials. *J. Mater. Chem.* **2001**, *11*, 37−53.
(16) Bramwell, S. T.; Gingras, M. J. P. Spin ice state in frustrated magnetic pyrochlore materials. *Science* **2001**, *294*, 1495−1501.
(17) Balents, L. Spin liquids in frustrated magnets. *Nature* **2010**, *464*, 199−208.
(18) Wosnitza, J.; Zvyagin, S. A.; Zherlitsyn, S. Frustrated magnets in high magnetic fields-selected examples. *Rep. Prog. Phys.* **2016**, *79*, No. 074504.
(19) Vojta, M. Frustration and quantum criticality. *Rep. Prog. Phys.* **2018**, *81*, No. 064501.
(20) Starykh, O. A. Unusual ordered phases of highly frustrated magnets: a review. *Rep. Prog. Phys.* **2015**, *78*, No. 052502.
(21) Schmidt, B.; Thalmeier, P. Frustrated two dimensional quantum magnets. *Phys. Rep.* **2017**, *703*, 1−59.
(22) Lee, S. H.; Takagi, H.; Louca, D.; Matsuda, M.; Ji, S.; Ueda, H.; Ueda, Y.; Katsufuji, T.; Chung, J.; Park, S.; Cheong, S.; Broholm, C. Frustrated magnetism and cooperative phase transitions in spinels. *J. Phys. Soc. Jpn.* **2010**, *79*, No. 011004.
(23) Tokura, Y.; Seki, S. Multiferroics with spiral spin orders. *Adv. Mater.* **2010**, *22*, 1554−1565.
(24) Ganguly, S.; Chimata, R.; Sanyal, B. Overcoming magnetic frustration and promoting half-metallicity in spinel $CoCr_2O_4$ by doping with Fe. *Phys. Rev. B: Condens. Matter Mater. Phys.* **2015**, *92*, 224417.
(25) Windsor, Y. W.; Piamonteze, C.; Ramakrishnan, M.; Scaramucci, A.; Rettig, L.; Huever, J. A.; Bothschafter, E. M.; Bingham, N. S.; Alberca, A.; Avula, S. R. V.; Noheda, B.; Staub, U. Magnetic properties of strained multiferroic $CoCr_2O_4$: A soft x-ray study. *Phys. Rev. B: Condens. Matter Mater. Phys.* **2017**, *95*, 224413.
(26) Heuver, J. A.; Scaramucci, A.; Blickenstorfer, Y.; Matzen, S.; Spaldin, N. A.; Ederer, C.; Noheda, B. Strain-induced magnetic anisotropy in epitaxial thin films of the spinel $CoCr_2O_4$. *Phys. Rev. B: Condens. Matter Mater. Phys.* **2015**, *92*, 214429.
(27) Aqeel, A.; Vlietstra, N.; Heuver, J. A.; Bauer, G. E. W.; Noheda, B.; van Wees, B. J.; Palstra, T. T. M. Spin-Hall magnetoresistance and spin Seebeck effect in spin-spiral and paramagnetic phases of multiferroic CoCr2O4 films. *Phys. Rev. B: Condens. Matter Mater. Phys.* **2015**, *92*, 224410.
(28) Kim, I.; Oh, Y.; Liu, Y.; Chun, S.; Lee, J.; Ko, K.; Park, J.; Chung, J.; Kim, K. Electric polarization enhancement in multiferroic $CoCr_2O_4$ crystals with Cr-site mixing. *Appl. Phys. Lett.* **2009**, *94*, No. 042505.
(29) Zhang, H. G.; Wang, Z.; Liu, E. K.; Wang, W. H.; Yue, M.; Wu, G. H. Site preference and compensation behavior in $Co(Cr, Mn)_2O_4$ system. *J. Appl. Phys.* **2015**, *117*, 17B735.
(30) Yang, S.; Bao, H. X.; Xue, D. Z.; Zhou, C.; Gao, J. H.; Wang, Y.; Wang, J. Q.; Song, X. P.; Sun, Z. B.; Ren, X. B.; Otsuka, K. Magnetodielectric effect from the onset of ferrimagnetic transition in $CoCr_2O_4$. *J. Phys. D: Appl. Phys.* **2012**, *45*, 265001.
(31) Guzman, R.; Heuver, J.; Matzen, S.; Magen, C.; Noheda, B. Structural and magnetic properties of [001] $CoCr_2O_4$ thin films. *Phys. Rev. B: Condens. Matter Mater. Phys.* **2017**, *96*, 104105.
(32) Chen, X.; Yang, Z.; Xie, Y.; Huang, Z.; Ling, L.; Zhang, S.; Pi, L.; Sun, Y.; Zhang, Y. Coexistence of incommensurate and commensurate spiral orders and pressure effect on polycrystalline $CoCr_2O_4$. *J. Appl. Phys.* **2013**, *113*, 17E129.
(33) Pronin, A. V.; Uhlarz, M.; Beyer, R.; Fischer, T.; Wosnitza, J.; Gorshunov, B. P.; Komandin, G. A.; Prokhorov, A. S.; Dressel, M.; Bush, A. A.; Torgashev, V. I. B-T phase diagram of $CoCr_2O_4$ in magnetic fields up to 14 T. *Phys. Rev. B: Condens. Matter Mater. Phys.* **2012**, *85*, No. 012101.
(34) Kocsis, V.; Bordács, S.; Varjas, D.; Penc, K.; Abouelsayed, A.; Kuntscher, C. A.; Ohgushi, K.; Tokura, Y.; Kézsmárki, I. Magneto-elasticity in ACr_2O_4 spinel oxides (A = Mn, Fe, Co, Ni, and Cu). *Phys. Rev. B: Condens. Matter Mater. Phys.* **2013**, *87*, No. 064416.
(35) Kamenskyi, D.; Engelkamp, H.; Fischer, T.; Uhlarz, M.; Wosnitza, J.; Gorshunov, B. P.; Komandin, G. A.; Prokhorov, A. S.; Dressel, M.; Bush, A. A.; Torgashev, V. I.; Pronin, A. V. Observation of an intersublattice exchange magnon in $CoCr_2O_4$ and analysis of magnetic ordering. *Phys. Rev. B: Condens. Matter Mater. Phys.* **2013**, *87*, 134423.
(36) Efthimiopoulos, I.; Liu, Z. T. Y.; Khare, S. V.; Sarin, P.; Lochbiler, T.; Tsurkan, V.; Loidl, A.; Popov, D.; Wang, Y. Pressure-induced transition in the multiferroic $CoCr_2O_4$ spinel. *Phys. Rev. B: Condens. Matter Mater. Phys.* **2015**, *92*, No. 064108.
(37) Tsurkan, V.; Zherlitsyn, S.; Yasin, S.; Felea, V.; Skourski, Y.; Deisenhofer, J.; von Nidda, H.-A. K.; Wosnitza, J.; Loidl, A. Unconventional magnetostructural transition in $CoCr_2O_4$ at high magnetic fields. *Phys. Rev. Lett.* **2013**, *110*, 115502.
(38) Lüders, U.; Sánchez, F.; Fontcuberta, J. Initial stages in the growth of (111)-faceted $CoCr_2O_4$ clusters: mechanisms and strained nanometric pyramides. *Appl. Phys. A: Mater. Sci. Process.* **2004**, *79*, 93−97.
(39) Lüders, U.; Sánchez, F.; Fontcuberta, J. Self-organized structures in $CoCr_2O_4$ (001) thin films: Tunable growth from pyramidal clusters to a (111) fully faceted surface. *Phys. Rev. B: Condens. Matter Mater. Phys.* **2004**, *70*, No. 045403.
(40) Lüders, U.; Sánchez, F.; Fontcuberta, J. Self-organized growth of pyramidal clusters in epitaxial spinel $CoCr_2O_4$ films on rock salt MgO (001) substrates. *Appl. Phys. A: Mater. Sci. Process.* **2005**, *81*, 103−108.
(41) Kaplan, T. A.; Dwight, K.; Lyons, D.; Menyuk, N. Classical theory of the ground spin state in spinels. *J. Appl. Phys.* **1961**, *32*, S13−S20.

DOI: 10.1021/acs.nanolett.9b02159
Nano Lett. 2019, 19, 8381−8387

(42) Lyons, D. H.; Kaplan, T. A.; Dwight, K.; Menyuk, N. Classical theory of the ground spin-state in cubic spinels. *Phys. Rev.* **1962**, *126*, 540−555.
(43) Yamasaki, Y.; Miyasaka, S.; Kaneko, Y.; He, J.-P.; Arima, T.; Tokura, Y. Magnetic reversal of the ferroelectric polarization in a multiferroic spinel oxide. *Phys. Rev. Lett.* **2006**, *96*, 207204.
(44) Choi, Y. J.; Okamoto, J.; Huang, D. J.; Chao, K. S.; Lin, H. J.; Chen, C. T.; van Veenendaal, M.; Kaplan, T. A.; Cheong, S.-W. Thermally or magnetically induced polarization reversal in the multiferroic $CoCr_2O_4$. *Phys. Rev. Lett.* **2009**, *102*, No. 067601.
(45) Dey, K.; Majumdar, S.; Giri, S. Ferroelectricity in spiral short-range-ordered magnetic state of spinel $MnCr_2O_4$: Significance of topological frustration and magnetoelastic coupling. *Phys. Rev. B: Condens. Matter Mater. Phys.* **2014**, *90*, 184424.
(46) Katsura, H.; Nagaosa, N.; Balatsky, A. V. Spin current and magnetoelectric effect in noncollinear magnets. *Phys. Rev. Lett.* **2005**, *95*, No. 057205.
(47) Sergienko, I. A.; Dagotto, E. Role of the Dzyaloshinskii-Moriya interaction in multiferroic perovskites. *Phys. Rev. B: Condens. Matter Mater. Phys.* **2006**, *73*, No. 094434.
(48) Tomiyasu, K.; Fukunaga, J.; Suzuki, K. Magnetic short-range order and reentrantspin-glass-like behavior in $CoCr_2O_4$ and $MnCr_2O_4$ by means of neutron scattering and magnetization measurements. *Phys. Rev. B: Condens. Matter Mater. Phys.* **2004**, *70*, 214434.
(49) Chang, L. J.; Huang, D. J.; Li, W.-H.; Cheong, S.-W.; Ratcliff, W.; Lynn, J. W. Crossover from incommensurate to commensurate magnetic orderings in $CoCr_2O_4$. *J. Phys.: Condens. Matter* **2009**, *21*, 456008.
(50) Yafet, Y.; Kittel, C. Antiferromagnetic arrangements in ferrites. *Phys. Rev.* **1952**, *87*, 290−294.
(51) Liu, X.; Choudhury, D.; Cao, Y.; Middey, S.; Kareev, M.; Meyers, D.; Kim, J.-W.; Ryan, P.; Chakhalian, J. Epitaxial growth of (111)-oriented spinel $CoCr_2O_4/Al_2O_3$ heterostructures. *Appl. Phys. Lett.* **2015**, *106*, No. 071603.
(52) Liu, X.; Kareev, M.; Cao, Y.; Liu, J.; Middey, S.; Meyers, D.; Freeland, J. W.; Chakhalian, J. Electronic and magnetic properties of (111)-oriented $CoCr_2O_4$ epitaxial thin film. *Appl. Phys. Lett.* **2014**, *105*, No. 042401.
(53) Kirby, B.J.; Kienzle, P.A.; Maranville, B.B.; Berk, N.F.; Krycka, J.; Heinrich, F.; Majkrzak, C.F. Phase-sensitive specular neutron reflectometry for imaging the nanometer scale composition depth profile of thin-film materials. *Curr. Opin. Colloid Interface Sci.* **2012**, *17*, 44−53.
(54) Thole, B. T.; Carra, P.; Sette, F.; van der Laan, G. X-ray circular dichroism as a probe of orbital magnetization. *Phys. Rev. Lett.* **1992**, *68*, 1943−1946.
(55) Carra, P.; Thole, B. T.; Altarelli, M.; Wang, X. X-ray circular dichroism and local magnetic fields. *Phys. Rev. Lett.* **1993**, *70*, 694−697.
(56) Chen, C. T.; Idzerda, Y. U.; Lin, H. J.; Smith, N. V.; Meigs, G.; Chaban, E.; Ho, G. H.; Pellegrin, E.; Sette, F. Experimental confirmation of the x-ray magnetic circular dichroism sum rules for iron and cobalt. *Phys. Rev. Lett.* **1995**, *75*, 152−155.
(57) Goering, E. X-ray magnetic circular dichroism sum rule correction for the light transition metals. *Philos. Mag.* **2005**, *85*, 2895−2911.
(58) Goodenough, J. B. *Magnetism and the Chemical Bond*; Interscience: New York, 1974.
(59) Vonsovskii, S. V. *Magnetism*; Wiley: New York, 1963; Vol. 2.
(60) For each sublattice below T_C, the net magnetization per site is given by the modified Brillouin function as proposed in refs 58 and 59: $y_i = B_{S_i}(x_i) = (2S_i + 1)/2S_i \coth((2S_i + 1)/2S_i x_i) - 1/2S_i \coth(1/2S_i x_i)$, where $y_i = M_i/M_{i0}$ and $x_i = (g_i\mu_B S_i/k_B T)[H + w(-a_i M_i - M_j)]$, $i \neq j$, where M_i is the magnetization per site of the ith sublattice, S_i is the spin magnetic moment of the ith sublattice, and M_{i0} is the saturated value of magnetization. In the $CoCr_2O_4$ system, $S_{Co} = S_{Cr} = 3/2$, and $g_{(Co)} = 2.2$ and $g_{(Cr)} = 2.0$.[70] Moreover, w in x_i represents the intersublattice Weiss constant, which is linearly proportional to the intersublattice exchange interaction $J_{Co\text{-}Cr}$, and a_i is the ratio of the intrasublattice exchange interaction with respect to the intersublattice value. The fit gives the value of intra- vs interexchange interaction $a_{Cr} = J_{Cr\text{-}Cr}/J_{Co\text{-}Cr} = 0.49 \pm 0.01$ and 0.37 ± 0.01 for $n = 4$ and 2 QL, respectively. More details about the fit can be found in the Supporting Information.
(61) Kang, J.-S.; Hwang, J.; Kim, D. H.; Lee, E.; Kim, W. C.; Kim, C. S.; Lee, H.; Kim, J.-Y.; Han, S. W.; Hong, S. C.; Kim, B.; Min, B. I. Soft x-ray magnetic circular dichroism study of valence and spin states in FeT_2O_4 (T = V, Cr) spinel oxides. *J. Appl. Phys.* **2013**, *113*, 17E116.
(62) Chung, J.; Song, Y.; Kim, J.-H.; Suzuki, T.; Katsufuji, T.; Matsuda, M.; Lee, S.-H. Dynamic spin correlations in the frustrated cubic phase of MnV_2O_4. *Phys. Rev. B: Condens. Matter Mater. Phys.* **2013**, *88*, No. 094430.
(63) Iwata-Harms, J.; Wong, F. J.; Alaan, U. S.; Kirby, B. J.; Borchers, J. A.; Toney, M. F.; Nelson-Cheeseman, B. B.; Liberati, M.; Arenholz, E.; Suzuki, Y. Controlling spin ordering in frustrated magnets via thin film heteroepitaxy. *Phys. Rev. B: Condens. Matter Mater. Phys.* **2012**, *85*, 214424.
(64) Menyuk, N.; Dwight, K.; Lyons, D.; Kaplan, T. A. Classical theory of the ground spin state in normal tetragonal spinels. I. Néel, Yafet-Kittel, and collinear antiferromagnetic modes. *Phys. Rev.* **1962**, *127*, 1983−1996.
(65) Willard, M. A.; Nakamura, Y.; Laughlin, D. E.; McHenry, M. E. Magnetic properties of ordered and disordered spinelphase ferrimagnets. *J. Am. Ceram. Soc.* **1999**, *82*, 3342−3346.
(66) Tsurkan, V.; Mücksch, M.; Fritsch, V.; Hemberger, J.; Klemm, M.; Klimm, S.; Körner, S.; von Nidda, H.-A. K.; Samusi, D.; Scheidt, E.-W.; Loidl, A.; Horn, S.; Tidecks, R. Magnetic, heat capacity, and conductivity studies of ferrimagnetic $MnCr_2S_4$ single crystals. *Phys. Rev. B: Condens. Matter Mater. Phys.* **2003**, *68*, 134434.
(67) Gillespie, R. J. Bond lengths and bond angles in octahedral, trigonal-bipyramidal, and related molecules of the non-transition elements. *Can. J. Chem.* **1961**, *39*, 318−323.
(68) Khomskii, D. *Transition Metal Compounds*; Cambridge University Press: Cambridge, 2014.
(69) Ederer, C.; Komelj, M. Magnetic coupling in $CoCr_2O_4$ and $MnCr_2O_4$: An LSDA + U study. *Phys. Rev. B: Condens. Matter Mater. Phys.* **2007**, *76*, No. 064409.
(70) Altshuler, S. A.; Kozyrev, B. M. *Electron Paramagnetic Resonance in Compounds of Transition Elements*; Wiley: New York, 1974.

DOI: 10.1021/acs.nanolett.9b02159
Nano Lett. 2019, 19, 8381−8387